AGU ADVANCING EARTH AND SPACE SCIENCES

Geophysical Research Letters®

RESEARCH LETTER
10.1029/2023GL104778

Special Section:
Years of the Maritime Continent

Westward-Propagating Disturbances Shape Diverse MJO Propagation

Yuntao Wei[1,2,3], **Hong-Li Ren**[2,4], **Wansuo Duan**[3], **and Guodong Sun**[3]

[1]Department of Atmospheric and Oceanic Sciences and Institute of Atmospheric Sciences, CMA-FDU Joint Laboratory of Marine Meteorology, Key Laboratory of Polar Atmosphere-ocean-ice System for Weather and Climate, Ministry of Education, Fudan University, Shanghai, China, [2]Collaborative Innovation Center on Forecast and Evaluation of Meteorological Disasters (CIC-FEMD), Nanjing University of Information Science and Technology, Nanjing, China, [3]LASG, Institute of Atmospheric Physics, Chinese Academy of Sciences, Beijing, China, [4]State Key Laboratory of Severe Weather, and Institute of Tibetan Plateau Meteorology, Chinese Academy of Meteorological Sciences, Beijing, China

Abstract Understanding eastward-propagating mechanisms of the Madden–Julian Oscillation (MJO) is of great importance for the subseasonal prediction of extreme weather and climate worldwide. Using global satellite observations and reanalysis data, this study unravels that dual combinations of strong/weak westward- (ISOw) and eastward-propagating intraseasonal oscillation (ISOe) can shape diverse MJO propagations documented previously using clustering analysis. The dry ISOw signals from the Central Pacific strengthen the leading suppressed convection over the Western Pacific (WP) and, on the contrary, weaken the moist ISOe convection over the Maritime Continent. Thus, when ISOe is weak over the WP, the strong (weak) dryness of ISOw likely causes a jump-like (stand-like) MJO mode. In contrast, a propagating MJO is supported when ISOe becomes strong over the WP, and a further strengthening of the ISOw dryness will presumably accelerate MJO; moreover, a weakening of ISOw might slow down the MJO speed.

Plain Language Summary Owing to the eastward propagation of the Madden–Julian Oscillation (MJO), tropical winds and precipitation usually oscillate in a broad life cycle of 20–100 days. The subseasonal (longer than 2 weeks but shorter than one season) prediction of extreme events, such as tropical cyclones, droughts, and heat waves, relies closely on an adequate understanding of the propagation mechanisms of MJO. Recently, clustering analysis has revealed four MJO propagation patterns, including stand, jump, slow, and fast modes. However, the underlying mechanisms of the origin of MJO propagation diversity are still elusive. Herein, we offer a novel explanation from the perspective of atmospheric westward-propagation disturbances (WPDs). These WPDs, which first appeared over the Central Pacific, can cause stand- and jump-like MJO modes when the eastward-propagating 20–100-day dry signals are weak over the Western Pacific. Otherwise, fast and slow MJO modes will be supported when the WPDs are further strengthened and weakened, respectively. These results highlight that the WPDs and their triggering place, that is, the Central Pacific, might serve as key ingredients for better understanding the MJO dynamics and predictability.

Key Points:

- Dual combinations of strong/weak westward- and eastward-propagating disturbances shape Madden–Julian Oscillation (MJO) diversity
- Westward-propagating disturbances control the formation of stand and jump MJOs and distinguish fast and slow MJOs
- Eastward-propagating disturbances primarily help MJO cross the Maritime Continent barrier

Supporting Information:

Supporting Information may be found in the online version of this article.

Correspondence to:

H.-L. Ren,
renhl@cma.gov.cn

Citation:

Wei, Y., Ren, H.-L., Duan, W., & Sun, G. (2023). Westward-propagating disturbances shape diverse MJO propagation. *Geophysical Research Letters*, *50*, e2023GL104778. https://doi.org/10.1029/2023GL104778

Received 31 MAY 2023
Accepted 27 AUG 2023

Author Contributions:

Conceptualization: Yuntao Wei
Formal analysis: Yuntao Wei
Investigation: Yuntao Wei
Methodology: Yuntao Wei
Project Administration: Hong-Li Ren
Resources: Hong-Li Ren, Wansuo Duan, Guodong Sun
Software: Yuntao Wei
Supervision: Hong-Li Ren
Validation: Yuntao Wei
Visualization: Yuntao Wei

1. Introduction

The Madden–Julian Oscillation (MJO) is the dominant mode of tropical intraseasonal variability with a broad time scale of 20–100 days (Zhang, 2005). Besides affecting local winds and precipitation, MJO can also greatly influence remote weather and climate through tropical–extratropical teleconnections (Stan et al., 2017; Zhang, 2013); hence, it serves as a major source of subseasonal-to-seasonal predictability (Vitart et al., 2017; Waliser et al., 2003). The fundamental characteristics and dynamics of MJO have been well-documented (Jiang et al., 2020; Zhang et al., 2020) since its first discovery (Madden & Julian, 1971, 1972). After being initiated from the Indian Ocean (IO) (Matthews, 2008; Wei et al., 2019, 2020, 2023; Zhao et al., 2013), MJO deep convection expands and migrates eastward slowly (~5 m/s) and may weaken when encountering the Maritime Continent (MC) barrier effect (Ling et al., 2019; Wei et al., 2022; Zhang & Ling, 2017); nevertheless, it can usually reintensify over the Western Pacific (WP) (Waliser et al., 2009; Wei & Pu, 2021) and finally damp over the Central-Eastern Pacific (Hendon & Salby, 1994; Wang & Chen, 2017; Wei et al., 2018).

However, observed MJO propagations are diverse in many aspects. For example, the MJO may propagate fast or slow (Pohl & Matthews, 2007; Yadav & Straus, 2017) under different modulations of low-frequency background states (Chen et al., 2022; Ren et al., 2023; Suematsu & Miura, 2022; Wang & Li, 2021; Wei & Ren, 2019, 2022;

Writing – original draft: Yuntao Wei
Writing – review & editing: Yuntao Wei, Hong-Li Ren, Wansuo Duan, Guodong Sun

Xiang et al., 2021). The propagating MJO may be blocked by the MC barrier effect (Barrett et al., 2021; Hirata et al., 2013; Zhang & Ling, 2017), which sometimes can be overcome by moistening arising from the leading suppressed convection (LSC) over the WP (Chen & Wang, 2018; Feng et al., 2015; Kim et al., 2014; Wei et al., 2022) or by reduced land diurnal cycle (Hagos et al., 2016; Ling et al., 2019; Oh et al., 2013). Additionally, MJO propagation trajectory (Kim et al., 2017; Liu et al., 2020; Zhou & Murtugudde, 2020) and group velocity (Wei et al., 2023; Wei & Ren, 2019) are changeable. Clustering analysis has been recently used to objectively identify diverse MJO propagations (Chen & Wang, 2021; Wang et al., 2021), such as standing, jumping, and slow eastward propagation and fast eastward propagation MJO modes (Wang et al., 2019, hereafter WCL19; Xiang et al., 2021; Wang & Wang, 2023). Although low-frequency variabilities, such as El Nino–Southern Oscillation (ENSO) and Quasi-Biennial Oscillation (Lyu et al., 2021; Wei et al., 2023; Xiang et al., 2021), likely control various MJO propagation behaviors, why diversified MJO propagations exist remains elusive.

Besides eastward-propagating intraseasonal oscillation (ISOe), westward-propagating intraseasonal oscillation (ISOw) is also active in the tropics, such as equatorial Rossby waves (Gonzalez & Jiang, 2019; Kiladis et al., 2009) or westward-propagating "moisture mode" (Fuchs-Stone et al., 2019; Mayta et al., 2022). Previous studies have noticed that ISOw might shape the boreal summer intraseasonal oscillation (Wang & Rui, 1990; Wang & Xie, 1997; Wang et al., 2021), anchor or initiate MJO deep convection by interplaying with high topography (Feng & Li, 2016; Roundy & Frank, 2004; Takasuka & Satoh, 2021; Wei et al., 2019, 2020, 2023), and block eastward propagation of MJO moist convection through dry intrusion (DeMott et al., 2018; Feng et al., 2015; Fu et al., 2018; Huang & Pegion, 2022). In this study, we unexpectedly found that ISOw, which cooperates with ISOe, over the WP, can offer a plausible explanation of diverse MJO propagation initiated from the IO (WCL19). Moreover, as an arguably key prerequisite for MJO eastward propagation (Chen & Wang, 2018; Feng et al., 2015; Kim et al., 2014; Wei & Ren, 2019), the LSC over the WP is found to be closely related to the ISOw. These results will be comprehensively described in Section 3 after an introduction of data and methodology in Section 2. Finally, we discuss our main findings and outline the conclusions in Section 4.

2. Data and Methodology

2.1. Data

The main data set used in this study is the daily, 2.5° × 2.5°, advanced very high-resolution radiometer outgoing longwave radiation (OLR) during 1979–2018 from the National Oceanic and Atmospheric Administration (NOAA; Liebmann & Smith, 1996). OLR is a good proxy of deep convection and rainfall in most tropical regions (Peatman et al., 2014). The atmospheric circulation is diagnosed using the 5th generation of ECMWF reanalysis (ERA5) products (Hersbach et al., 2020). Daily anomalies are calculated by subtracting calendar daily climatology. A 20–100-day bandpass Lanczos filter (Duchon, 1979) with 201 weights is used to extract the intraseasonal oscillation (ISO) from the daily anomalies. The westward and eastward components of ISO (i.e., ISOw and ISOe) are further extracted using the Fourier and inverse-Fourier transforms along each latitude.

2.2. Methodology

We first derive a convective index (CI), defined as the ISO component of OLR averaged over the IO (15°S–15°N, 70°–100°E). The reference date (hereafter, Day 0) is selected as the first day when CI becomes smaller than one negative standard deviation (STD) of itself. The composite map for the total ISO component of OLR shows enhanced convective anomalies in the central IO and suppressed convective anomalies in the WP (Figure S1 in Supporting Information S1). Thus, we further derive a dry index (DI) following Kim et al. (2014) as the ISO component of OLR averaged over the WP (15°S–15°N, 120°E−180°E). The large scatter of DI, relative to the small CI scatter (Figure 1a), suggests that the LSC defined by the DI can be independent of the MJO moist convection over the IO. Kim et al. (2014) revealed that strong LSC could support a propagating MJO, while weak LSC usually corresponds to a nonpropagating MJO. This is reproduced in Figure S2 in Supporting Information S1. Here, "Strong" ("Weak") is defined as the scenario when DI is larger (smaller) than the mean plus (minus) half of its STD.

We further decompose DI into ISOe and ISOw components to quantify the relative LSC contributions from eastward- and westward-propagating disturbances. Again, there exists no clear linear relation between CI and the two DI components (Figure 1b). However, the total DI is considerably correlated with its two components

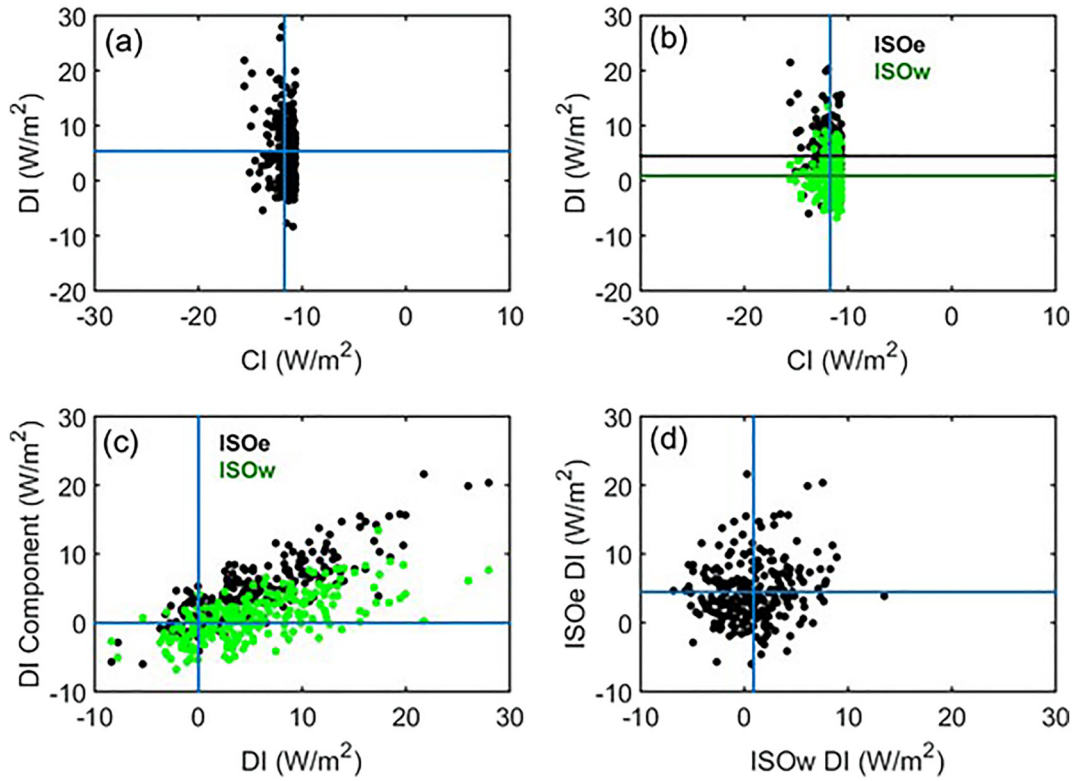

Figure 1. Dry and convective indices (DI and CI). (a) Scatter diagram of CI versus DI derived as the 20–100-day-filtered OLR anomalies (W/m^2) over the Western Pacific (15°S–15°N, 120°E–180°E). The horizontal (vertical) blue line is the mean of DI (CI). (b) Same as (a) but for the CI versus ISOe (black) and ISOw (green) components of DI. The black and green horizontal lines denote the means of ISOe and ISOw. (c) Scatter diagram of DI versus its two components of ISOe and ISOw. (d) Scatter diagram of ISOw versus ISOe components of DI.

(Figure 1c), and the dryness over the WP is mainly contributed by ISOe as the magnitude of ISOe is larger than ISOw. The LSC over the WP is a robust signal of eastward-propagating MJO, both in the successive- and primary-type events (Chen & Wang, 2018; Matthews, 2008). Here, we reveal that besides the preceding eastward-propagating dry anomalies, ISOw also contributes to the LSC (Wei et al., 2023). More interestingly, ISOw and ISOe are largely independent (Figure 1d). Thus, we can readily investigate their separate roles in affecting MJO eastward propagation.

Specifically, we define four scenarios based on the strength of ISOw and ISOe over the WP on Day 0. In the first scenario (**S-I**), both ISOw and ISOe are weak; in the second scenario (**S-II**), ISOe is weak, but ISOw is strong; in the third (**S-III**) and fourth (**S-IV**) scenarios, ISOe is strong, while ISOw is respectively weak and strong. The definitions of "Strong" and "Weak" are similar to the total DI. The equatorially (15°S–15°N) averaged convection and circulation anomalies of total ISO are composited in each scenario to examine the propagation pattern of MJO initiated from the IO. The composite of ISOw and ISOe components diagnoses the underlying mechanisms of distinct MJO propagation behaviors. The significance of composite results is evaluated based on the two-tailed Student-*t* test at the 95% confidence level. We consider the all-seasonal analysis to make a fair comparison with previous studies (e.g., Kim et al., 2014; Wei et al., 2023). In the represented results, seasonal variations, if any, are discussed somewhere in the following.

3. Results

3.1. MJO Propagation Under Weak Versus Strong ISOe

We first observe the MJO behaviors when only referring to the ISOe component of LSC over the WP. The maps of 20–100-day-filtered OLR and 850-hPa horizontal winds (UV850) on Day 0 are shown in Figures S3a and S3b in Supporting Information S1. As expected, the LSC in the strong ISOe case is considerably stronger than in the

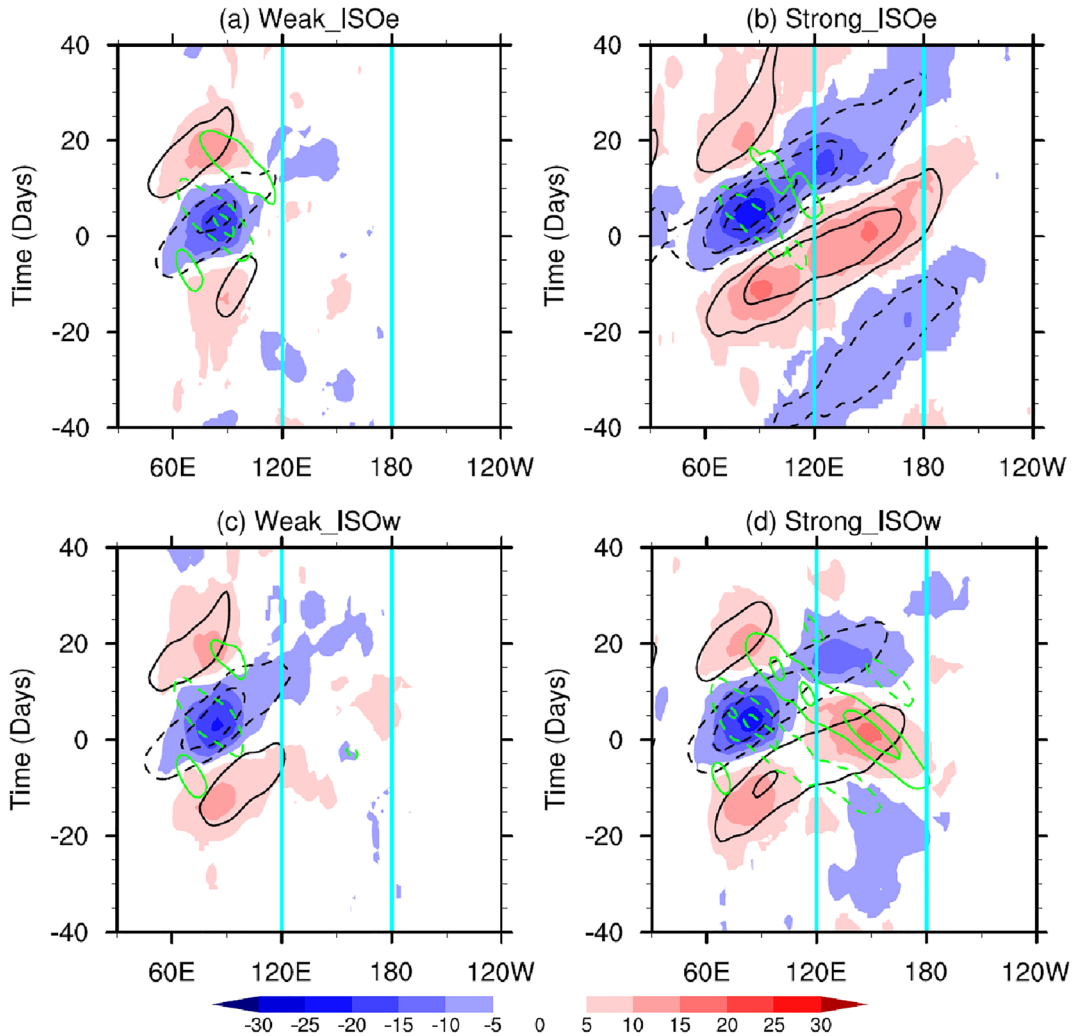

Figure 2. MJO propagation patterns conditioned by only ISOe or ISOw. (a) Lagged composite Hovmöller diagram of equatorial (15°S–15°N average), 20–100-day-filtered OLR anomalies (shading in W/m^2, passing the Student-*t* test at 95% confidence level) when only the ISOe component of leading suppressed convection is weak. (b–d) Same as (a) but for strong ISOw, weak ISOw, and strong ISOw, respectively. The black contours show the ISOe component, and the green contours are the ISOw component. Solid (dashed) contours denote suppressed (enhanced) convection, and zero contours are omitted. "Strong" is defined as larger than one plus half of the STD, while "Weak" is smaller than one minus half of the STD. The two cyan lines show the west and east boundaries of the WP. The MJO case numbers in the four panels are 64, 79, 74, and 76, respectively.

weak ISOe case. The strong LSC over the WP excites anticyclone Rossby gyres to the west (Gill, 1980), of which the poleward wind anomalies are observed, in contrast to the equator-ward winds in the weak ISOe case. Additionally, the equatorial easterly wind anomalies are considerably strengthened, mainly due to the dry Rossby wave excitation. Moreover, the suppressed convection of ISOe maximizes along the equator when it propagates into the WP on Day 0 during both boreal winter and summer (Figure S4 in Supporting Information S1), thus explaining the equatorially symmetric feature of the LSC in the ISOe component (Figure S3b in Supporting Information S1). The anomalous convection and circulation are generally similar to that based on the total LSC (Figures S1b and S1c in Supporting Information S1), which implies that weak (strong) LSC over the WP is mainly because of the weakening (strengthening) of ISOe.

The contrasting circulation between the two scenarios sheds some light on the different propagation patterns of MJO (Figures 2a and 2b). In the weak ISOe case, the deep convection is initiated from the western IO on Day −10, then migrates to the eastern IO with significantly enhanced amplitude, and quickly damps upon approaching Sumatra Island in the western MC. Therefore, a non-propagating (or a stand) MJO probably commences when

the suppressed convection of ISOe becomes weakened over the WP. In contrast, in the strong ISOe case, the deep convection successfully crosses the MC barrier and even reintensifies over the WP, manifesting a typical life cycle of propagating MJO. Two mechanisms have been previously used to explain the propagating MJO related to strong LSC. (a) The easterly winds induce boundary layer moisture convergence (Chen & Wang, 2018), and (b) the poleward winds cause positive meridional moisture advection (Kim et al., 2014; Wei & Ren, 2019). Both mechanisms helped MJO cross the MC barrier. Thus, the dryness of ISOe over the WP mainly determines whether the MJO can propagate eastward, thereby crossing the MC.

3.2. MJO Propagation Under Weak Versus Strong ISOw

What is the role of the WP dryness arising from ISOw? To answer this question, we examine the LSC and UV850 (Figures S3c and S3d in Supporting Information S1) as well as MJO propagation (Figures 2c and 2d) by defining "Strong" and "Weak" cases based only on the ISOw component. Again, we yield significantly stronger LSC and easterly/poleward wind anomalies in the strong ISOw case than in the weak ISOw case. However, this cannot be treated as a duplicate of Figures S3a and S3b in Supporting Information S1. In the weak ISOw case (Figure S3c in Supporting Information S1), suppressed convection of ISOe, albeit weak, is still observed in southern WP, causing stronger easterly wind anomalies along ∼10°S compared to the weak ISOe case (Figure S3a in Supporting Information S1). The underlying reason is that constraining ISOw to be weak does not necessarily guarantee a weak ISOe because the two components are largely independent (Figure 1d). Moreover, in the strong ISOw case, the LSC and the induced wind responses to the south of the equator are weak because the dryness of ISOw, as a major contributor to LSC, reaches a maximum in the north of the equator (Figure S3d in Supporting Information S1). The dry signals of ISOw are mainly seen along 10°N, although featuring westward propagation in boreal winter and northwestward propagation in boreal summer (Figure S5 in Supporting Information S1). We found that the LSC in the ISOw component in boreal summer is stronger than in boreal winter (Figure S6 in Supporting Information S1). Besides, in this case, both the easterly and poleward wind anomalies over the MC (especially those over the southern MC) are weaker than the strong ISOe case (Figure S3b in Supporting Information S1).

The deep convection over the IO in the weak ISOw case (Figure 2c) displays a similar propagation pattern as that in the weak ISOe case (Figure 2a). The major difference is that the damping of moist convection over the western MC in Figure 2c is not that strong. Consequently, the MJO convection can continuously propagate into the WP, but without reintensification. Therefore, a propagating mode is supported in the weak ISOw case. In the strong ISOw case, a westward-propagating disturbance initiated from the Central Pacific (CP) is observed (Figure 2d). The dry phase, on the one hand, strengthens the LSC over the WP on Day 0 and, on the other hand, suppresses the enhanced convection over the MC on Day 10. Because of the strong LSC, the in situ active convection over the WP is intensified after Day 10. In general, the MJO, in this case, behaves as a mixture of jumping and propagating modes. Moreover, MJO propagation speed tends to be slow in the weak ISOw case but fast in the strong ISOw case. Also note that, the moist phase of ISOw in the strong ISOw case propagates westward and helps to trigger the MJO deep convection from the IO, which is essentially like the WPISO type of MJO initiation documented by Wei et al. (2023) using clustering analysis.

Hence, we can see that more stories can be detected when isolating the ISOw component from the total LSC over the WP. To exclude the contamination of ISOe and thus extract the "pure" effect of ISOw, we then compare the LSC, UV850, and MJO propagation by constraining both the ISOw and ISOe components in the following subsection.

3.3. ISOw Cooperating With ISOe Shapes Diverse MJO Propagations

Figure 3 shows the 20–100-day-filtered UV850, OLR, and the ISOw and ISOe components in the four scenarios mentioned above (i.e., **S-I** to **S-IV**). In **S-I**, the northern WP interestingly displays weak active convection, and northerly wind anomalies are observed over northern MC, in contrast to weak southerly winds in southern MC (Figure 3a). In **S-II**, ISOw becomes strong, and significant convective suppression appears in northern WP (Figure 3b), thereby exciting southerly and easterly wind anomalies over northern MC (Figure 3b). In **S-III** and **S-IV**, owing to the dominance of ISOe, the suppressed convection over the WP becomes more symmetric about the equator and stronger (Figures 3c and 3d), which is more so in **S-IV** due to the further strengthened ISOw component (Figure 3d). Correspondingly, the spatial scale (both zonal and meridional) and amplitude of

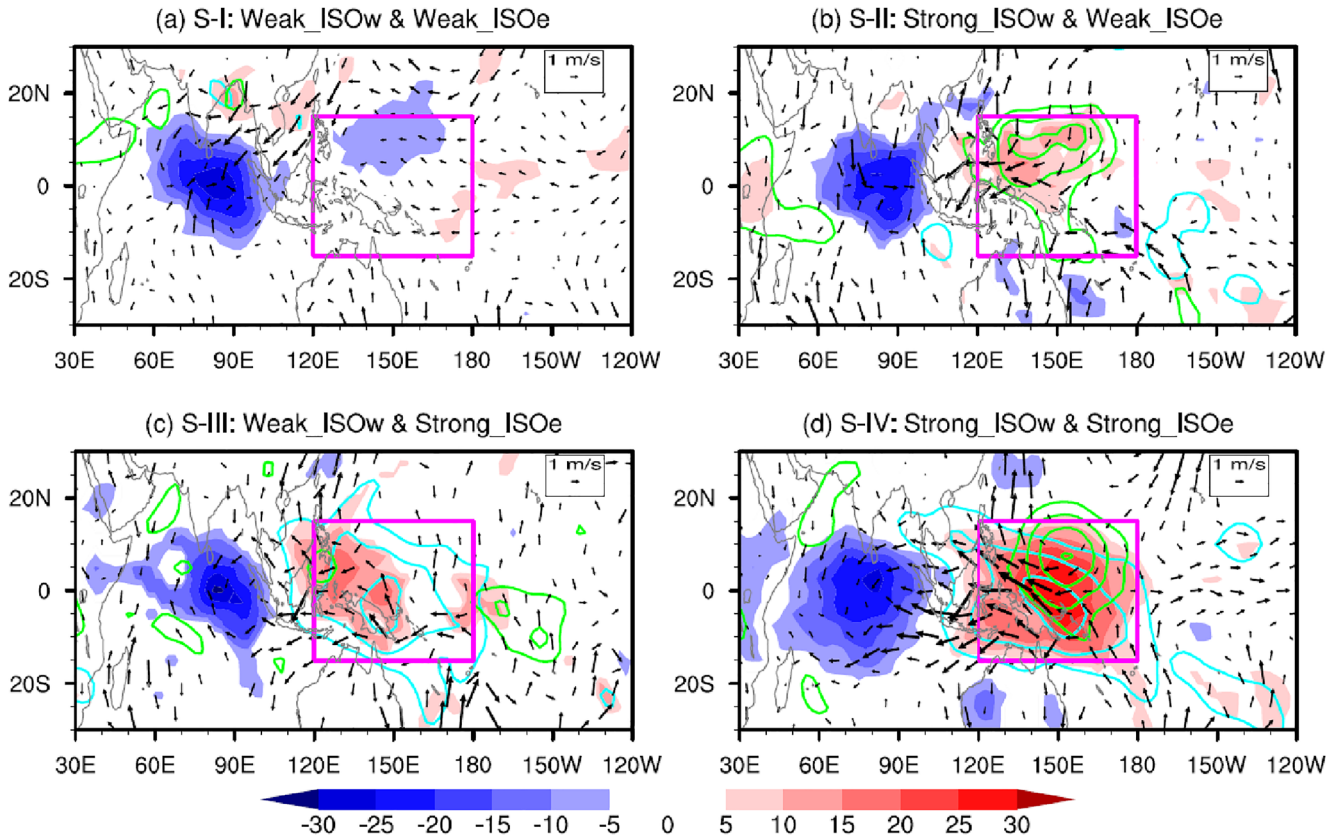

Figure 3. LSC conditioned by both ISOe and ISOw. (a) Composite 20–100-day-filtered OLR anomalies (shading in W/m^2 and passing the Student-*t* test at the 95% confidence level) as well as their westward- (ISOw, green contours) and eastward-propagating (ISOe, cyan contours) components on Day 0 in **S-I** (weak ISOw and weak ISOe). The contours are only shown for the suppressed convection. The vectors are the 850-hPa horizontal winds. The magenta rectangle encloses the box (15°S–15°N, 120°E−180°E) to calculate the LSC over the WP. (b–d) Same as (a) but for **S-II** (strong ISOw and weak ISOe), **S-III** (weak ISOw and strong ISOe), and **S-IV** (strong ISOw and strong ISOe), respectively. See texts for the definitions of **S-I** to **S-IV**. The MJO case numbers in the four panels are 33, 15, 13, and 30, respectively.

lower-tropospheric winds largely increase, especially in **S-IV**. Note that the amplitude of deep convection over the IO is generally similar in the four scenarios; therefore, the increasing lower-level wind amplitude mainly reflects the strengthening Rossby wave responses to the LSC over the WP. The "pure" effect of, say ISOw, might be appreciated by comparing such as **S-III** and **S-IV**. Because the significant contribution of LSC is ISOe, we expect that the so-derived "pure" ISOe effect (e.g., **S-I** vs. **S-III** comparison) is roughly the same as that in Section 3.1.

Figure 4 shows the MJO propagation patterns of the four scenarios. In **S-I** (Figure 4a), convective anomalies only oscillate over the IO with a time scale of 30–40 days but without a robust eastward propagation into the WP (see the break at 110°E), which is reminiscent of the standing MJO mode documented by WCL19. This non-propagating behavior is mainly attributed to the phase locking of ISOw and ISOe over the IO, both of which have similar amplitude but features opposite propagation direction. Roundy and Frank (2004) also reported a similar standing feature of ISO, which they called "resonant" wave interactions. In **S-II** (Figure 4b), a strong dry signal of ISOw propagates westward from the CP, hindering the further eastward expansion of the eastward-propagating moist signal of ISOe from the IO. This decaying mechanism of the MC barrier effect due to westward-propagating dry wave is also documented previously (DeMott et al., 2018; Feng et al., 2015; Huang & Pegion, 2022). Interestingly, significant moist convection reappears over the WP immediately following the dry ISOw signal. Overall, the propagation pattern in **S-II** is similar to the Jump MJO mode in WCL19.

A propagating mode can be observed in **S-III** and **S-IV** because the dryness arising from ISOe is strong over the WP. In **S-III** (Figure 4c), the ISOw signals mainly exist over the IO while weak over the WP. Similar to **S-II**, in **S-IV**, a westward-propagating dry signal of ISOw is observed, which propagates into the WP and strengthens

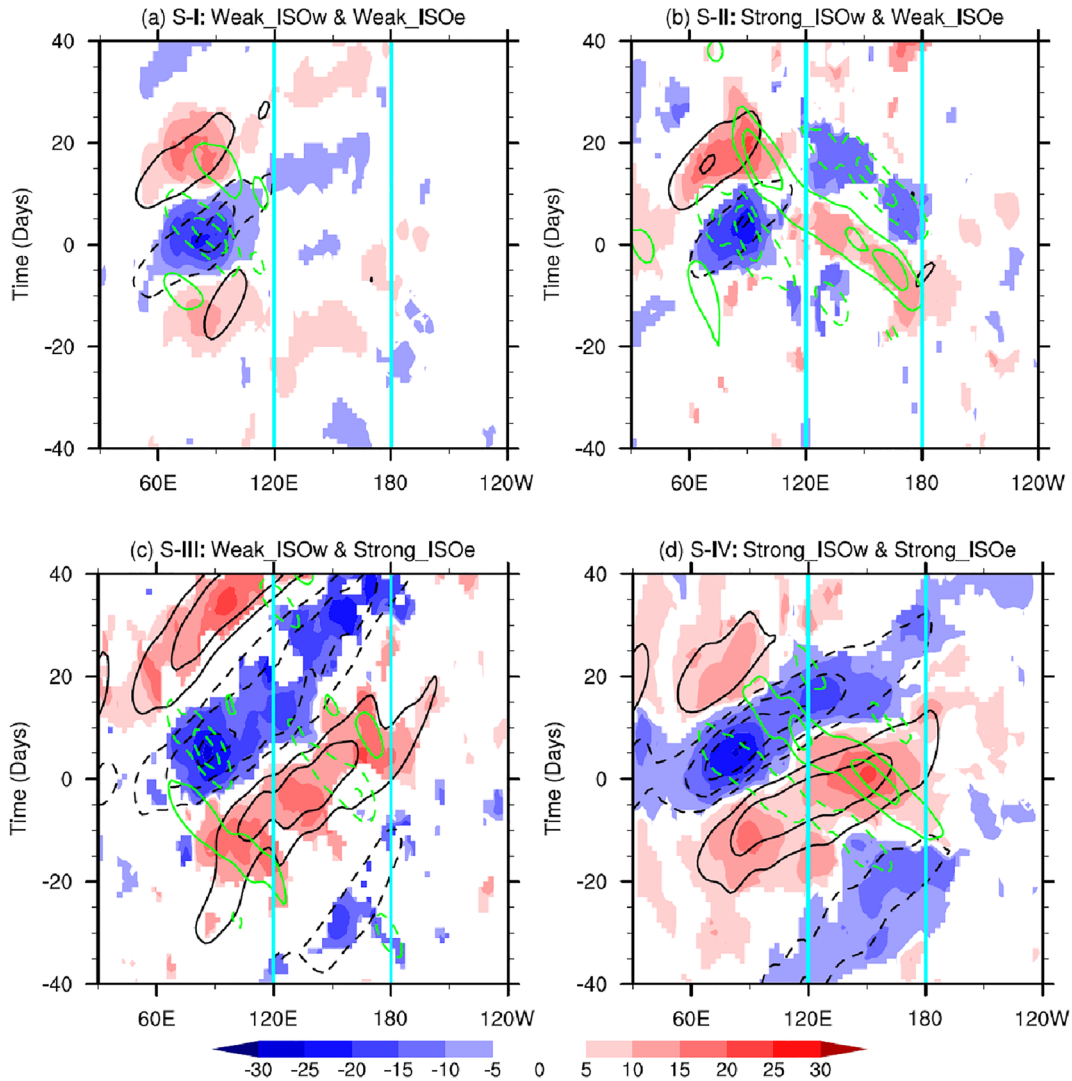

Figure 4. Same as Figure 2 but for the MJO propagation patterns conditioned by both ISOe and ISOw.

the in situ LSC (Figure 4d). However, the dry signal cannot propagate further west as in **S-II** because it is quickly damped by the moist convection of ISOe over the MC. The most attractive difference between **S-III** and **S-IV** is the propagation speed, which is slow in **S-III** and fast in **S-IV**. Thus, when the moist convection triggered from the IO can smoothly propagate across the MC (due mainly to the strong ISOe), the arrival of a westward-propagating dry signal over the WP will speed up the eastward-propagating moist convection (i.e., fast MJO); otherwise, a slow MJO will be supported. The crucial importance of ISOw in shaping the MJO diversity was further discussed in Text S1 in Supporting Information S1.

4. Discussion and Conclusion

4.1. Discussion

The results of this study have implications for the further development of the MJO theory (Zhang et al., 2020). Many popular MJO theories have intensively tried to simulate ISOe-like mode (Adames & Kim, 2016; Wang et al., 2016). However, according to the results of our study, along with previous studies, ISOw is also equally important to obtain a full paradigm of MJO propagation. A stochastically or interannually modulated onset or demise of ISOw in theoretical models should facilitate the formation of diverse MJO propagation as in reality. As a good candidate, the "MJO skeleton" model can simulate both ISOw and ISOe (Majda & Stechmann, 2009),

and the addition of a random process captures the irregularity of MJO initiation (Thual et al., 2014). However, whether the MJO propagation diversity was successfully reproduced in such stochastical models has not been examined.

The ISOw triggered from the CP has now been revealed to be crucial in shaping diverse MJO initiation and propagation. Thus, the CP, which previously was less concerned, is likely a key region to understand MJO dynamics and predictability. Wei et al. (2019) successfully predicted strong primary MJO initiation 10–15 days in advance by adding optimal moisture perturbations over the IO, which was motivated by the DYNAMO field campaign (Zhang & Yoneyama, 2017). Thus, what if we consider the optimal initiation over the CP? Will the prediction skill of MJO initiation and/or propagation be extended, considering that the ISOw signal can be tracked earlier over the CP? Wei et al. (2023) found that by helping MJO convective initiation over the IO, the ISOw precursor signals from the CP can increase the predictability of primary MJO events by 1 week, compared with other primary MJO initiations without the ISOw preconditioning. Addressing these questions is of great and practical importance for the MJO target observation and ensemble prediction.

4.2. Concluding Remarks

A growing number of studies have recently discovered diversity in MJO propagation, which has advanced our understanding of the fundamental dynamics of MJO, a mysterious phenomenon prevailing in the tropics and greatly influencing global weather and climate (Hand, 2015). However, a comprehensive explanation of the origin of different MJO propagations still needs to be discovered. Herein, we observed that the diverse MJO propagation patterns can be physically reproduced by examining the amplitude variation in the WP dry signals of ISOw triggered from the CP. More specifically, when ISOe does not bring in strong LSC over the WP, a westward-propagating dry signal of ISOw will facilitate the formation of Jumping MJO mode. Moreover, when the ISOw dry signal is weak, a standing MJO mode may appear. In contrast, when the dryness from ISOe is strong over the WP, the dry ISOw signal will mainly affect the MJO propagation speed, which generally increases with the strengthening of ISOw. Therefore, the variations of westward-propagating intraseasonal disturbances from the CP may help shape diverse MJO propagations (WCL19) under cooperation with the eastward-propagating intraseasonal disturbances from the IO. By considering the modulation effects of ENSO, we added an extended discussion of the importance of ISOw-ISOe interactions in understanding MJO propagation in Text S2 in Supporting Information S1.

Data Availability Statement

The OLR data was from the NOAA/OAR/ESRL PSD, Boulder, Colorado (Liebmann & Smith, 1996), available at https://psl.noaa.gov/thredds/catalog/Datasets/interp_OLR/catalog.html. The ERA5 reanalysis data (Hersbach et al., 2020) was available at https://doi.org/10.24381/cds.bd0915c6. The NOAA ERSSTv5 (Huang et al., 2017) was available at https://psl.noaa.gov/data/gridded/data.noaa.ersst.v5.html.

Acknowledgments
We thank the two anonymous reviewers that help improve the paper. This study is jointly supported by the National Natural Science Foundation of China (Grants 42288101 and U2242206). Y. Wei thanks the funding support of LASG.

References

Adames, Á. F., & Kim, D. (2016). The MJO as a dispersive, convectively coupled moisture wave: Theory and observations. *Journal of the Atmospheric Sciences*, *73*(3), 913–941. https://doi.org/10.1175/jas-d-15-0170.1

Barrett, B. S., Densmore, C. R., Ray, P., & Sanabia, E. R. (2021). Active and weakening MJO events in the Maritime Continent. *Climate Dynamics*, *57*(1–2), 157–172. https://doi.org/10.1007/s00382-021-05699-8

Chen, G., Ling, J., Zhang, Y., Wang, X., & Li, C. (2022). MJO propagation over the Indian Ocean and Western Pacific in CMIP5 models: Roles of background states. *Journal of Climate*, *35*(3), 955–973.

Chen, G., & Wang, B. (2018). Effects of enhanced front walker cell on the eastward propagation of the MJO. *Journal of Climate*, *31*(19), 7719–7738. https://doi.org/10.1175/jcli-d-17-0383.1

Chen, G., & Wang, B. (2021). Diversity of the boreal summer intraseasonal oscillation. *Journal of Geophysical Research: Atmospheres*, *126*(8), e2020JD034137. https://doi.org/10.1029/2020jd034137

DeMott, C. A., Wolding, B. O., Maloney, E. D., & Randall, D. A. (2018). Atmospheric mechanisms for MJO decay over the Maritime Continent. *Journal of Geophysical Research: Atmospheres*, *123*(10), 5188–5204. https://doi.org/10.1029/2017jd026979

Duchon, C. E. (1979). Lanczos filtering in one and two dimensions. *Journal of Applied Meteorology and Climatology*, *18*(8), 1016–1022. https://doi.org/10.1175/1520-0450(1979)018<1016:lfioat>2.0.co;2

Feng, J., & Li, T. (2016). Initiation mechanisms for a successive MJO event and a primary MJO event during boreal winter of 2000-2001. *Journal of Tropical Meteorology*, *22*(4).

Feng, J., Li, T., & Zhu, W. (2015). Propagating and nonpropagating MJO events over Maritime Continent. *Journal of Climate*, *28*(21), 8430–8449. https://doi.org/10.1175/jcli-d-15-0085.1

Fu, J. X., Wang, W., Ren, H. L., Jia, X., & Shinoda, T. (2018). Three different downstream fates of the boreal-summer MJOs on their passages over the Maritime Continent. *Climate Dynamics*, *51*(5–6), 1841–1862. https://doi.org/10.1007/s00382-017-3985-2

Fuchs-Stone, Ž., Raymond, D. J., & Sentić, S. (2019). A simple model of convectively coupled equatorial Rossby waves. *Journal of Advances in Modeling Earth Systems*, *11*(1), 173–184. https://doi.org/10.1029/2018ms001433

Gill, A. E. (1980). Some simple solutions for heat-induced tropical circulation. *Quarterly Journal of the Royal Meteorological Society*, *106*(449), 447–462. https://doi.org/10.1002/qj.49710644905

Gonzalez, A. O., & Jiang, X. (2019). Distinct propagation characteristics of intraseasonal variability over the tropical west Pacific. *Journal of Geophysical Research: Atmospheres*, *124*(10), 5332–5351. https://doi.org/10.1029/2018jd029884

Hagos, S. M., Zhang, C., Feng, Z., Burleyson, C. D., De Mott, C., Kerns, B., et al. (2016). The impact of the diurnal cycle on the propagation of Madden-Julian Oscillation convection across the Maritime Continent. *Journal of Advances in Modeling Earth Systems*, *8*(4), 1552–1564. https://doi.org/10.1002/2016ms000725

Hand, E. (2015). The storm king. *Science*, *350*(6256), 22–25. https://doi.org/10.1126/science.350.6256.22

Hendon, H. H., & Salby, M. L. (1994). The life cycle of the Madden–Julian oscillation. *Journal of the Atmospheric Sciences*, *51*(15), 2225–2237. https://doi.org/10.1175/1520-0469(1994)051<2225:tlcotm>2.0.co;2

Hersbach, H., Bell, B., Berrisford, P., Hirahara, S., Horányi, A., Muñoz-Sabater, J., et al. (2020). The ERA5 global reanalysis. *Quarterly Journal of the Royal Meteorological Society*, *146*(730), 1999–2049. https://doi.org/10.1002/qj.3803

Hirata, F. E., Webster, P. J., & Toma, V. E. (2013). Distinct manifestations of austral summer tropical intraseasonal oscillations. *Geophysical Research Letters*, *40*(12), 3337–3341. https://doi.org/10.1002/grl.50632

Huang, B., Thorne, P. W., Banzon, V. F., Boyer, T., Chepurin, G., Lawrimore, J. H., et al. (2017). Extended reconstructed sea surface temperature, version 5 (ERSSTv5): Upgrades, validations, and intercomparisons. *Journal of Climate*, *30*(20), 8179–8205. https://doi.org/10.1175/jcli-d-16-0836.1

Huang, K., & Pegion, K. (2022). The roles of westward-propagating waves and the QBO in limiting MJO propagation. *Journal of Climate*, *35*(18), 6031–6049. https://doi.org/10.1175/jcli-d-21-0691.1

Jiang, X., Adames, Á. F., Kim, D., Maloney, E. D., Lin, H., Kim, H., et al. (2020). Fifty years of research on the Madden-Julian Oscillation: Recent progress, challenges, and perspectives. *Journal of Geophysical Research: Atmospheres*, *125*(17), e2019JD030911. https://doi.org/10.1029/2019jd030911

Kiladis, G. N., Wheeler, M. C., Haertel, P. T., Straub, K. H., & Roundy, P. E. (2009). Convectively coupled equatorial waves. *Reviews of Geophysics*, *47*(2). https://doi.org/10.1029/2008rg000266

Kim, D., Kim, H., & Lee, M. I. (2017). Why does the MJO detour the Maritime Continent during austral summer? *Geophysical Research Letters*, *44*(5), 2579–2587. https://doi.org/10.1002/2017gl072643

Kim, D., Kug, J. S., & Sobel, A. H. (2014). Propagating versus nonpropagating Madden–Julian oscillation events. *Journal of Climate*, *27*(1), 111–125. https://doi.org/10.1175/jcli-d-13-00084.1

Liebmann, B., & Smith, C. A. (1996). Description of a complete (interpolated) outgoing longwave radiation data set. *Bulletin of the American Meteorological Society*, *77*(6), 1275–1277.

Ling, J., Zhang, C., Joyce, R., Xie, P. P., & Chen, G. (2019). Possible role of the diurnal cycle in land convection in the barrier effect on the MJO by the Maritime Continent. *Geophysical Research Letters*, *46*(5), 3001–3011. https://doi.org/10.1029/2019gl081962

Liu, J., Da, Y., Li, T., & Hu, F. (2020). Impact of ENSO on MJO pattern evolution over the Maritime Continent. *Journal of Meteorological Research*, *34*(6), 1151–1166. https://doi.org/10.1007/s13351-020-0046-2

Lyu, M., Jiang, X., Wu, Z., Kim, D., & Adames, Á. F. (2021). Zonal-scale of the Madden-Julian Oscillation and its propagation speed on the interannual time-scale. *Geophysical Research Letters*, *48*(6), e2020GL091239. https://doi.org/10.1029/2020gl091239

Madden, R. A., & Julian, P. R. (1971). Detection of a 40-50 day oscillation in the zonal wind in the tropical Pacific. *Journal of the Atmospheric Sciences*, *28*(5), 702–708. https://doi.org/10.1175/1520-0469(1971)028<0702:doadoi>2.0.co;2

Madden, R. A., & Julian, P. R. (1972). Description of global-scale circulation cells in the tropics with a 40-50 day period. *Journal of the Atmospheric Sciences*, *29*(6), 1109–1123. https://doi.org/10.1175/1520-0469(1972)029<1109:dogscc>2.0.co;2

Majda, A. J., & Stechmann, S. N. (2009). The skeleton of tropical intraseasonal oscillations. *Proceedings of the National Academy of Sciences*, *106*(21), 8417–8422. https://doi.org/10.1073/pnas.0903367106

Matthews, A. J. (2008). Primary and successive events in the Madden–Julian Oscillation. *Quarterly Journal of the Royal Meteorological Society*, *134*(631), 439–453. https://doi.org/10.1002/qj.224

Mayta, V. C., Adames, Á. F., & Ahmed, F. (2022). Westward-propagating moisture mode Over the tropical Western Hemisphere. *Geophysical Research Letters*, *49*(6), e2022GL097799. https://doi.org/10.1029/2022gl097799

Oh, J. H., Kim, B. M., Kim, K. Y., Song, H. J., & Lim, G. H. (2013). The impact of the diurnal cycle on the MJO over the Maritime Continent: A modeling study assimilating TRMM rain rate into global analysis. *Climate Dynamics*, *40*(3–4), 893–911. https://doi.org/10.1007/s00382-012-1419-8

Peatman, S. C., Matthews, A. J., & Stevens, D. P. (2014). Propagation of the Madden-Julian Oscillation through the Maritime Continent and scale interaction with the diurnal cycle of precipitation. *Quarterly Journal of the Royal Meteorological Society*, *140*(680), 814–825. Portico. https://doi.org/10.1002/qj.2161

Pohl, B., & Matthews, A. J. (2007). Observed changes in the lifetime and amplitude of the Madden-Julian Oscillation associated with interannual ENSO sea surface temperature anomalies. *Journal of Climate*, *20*(11), 2659–2674. https://doi.org/10.1175/jcli4230.1

Ren, H. L., Wei, Y., & Zhao, S. (2023). Low-frequency variability in the real-time multivariate MJO index: Real or artificial? *Journal of Climate*, *36*(7), 2073–2089. https://doi.org/10.1175/jcli-d-22-0368.1

Roundy, P. E., & Frank, W. M. (2004). Effects of low-frequency wave interactions on intraseasonal oscillations. *Journal of the Atmospheric Sciences*, *61*(24), 3025–3040. https://doi.org/10.1175/jas-3348.1

Stan, C., Straus, D. M., Frederiksen, J. S., Lin, H., Maloney, E. D., & Schumacher, C. (2017). Review of tropical-extratropical teleconnections on intraseasonal time scales. *Reviews of Geophysics*, *55*(4), 902–937. https://doi.org/10.1002/2016rg000538

Suematsu, T., & Miura, H. (2022). Changes in the eastward movement speed of the Madden–Julian oscillation with fluctuation in the Walker circulation. *Journal of Climate*, *35*(1), 211–225.

Takasuka, D., & Satoh, M. (2021). Diversity of the Madden–Julian oscillation: Initiation region modulated by the interaction between the intraseasonal and interannual variabilities. *Journal of Climate*, *34*(6), 2297–2318. https://doi.org/10.1175/jcli-d-20-0688.1

Thual, S., Majda, A. J., & Stechmann, S. N. (2014). A stochastic skeleton model for the MJO. *Journal of the Atmospheric Sciences*, *71*(2), 697–715. https://doi.org/10.1175/jas-d-13-0186.1

Vitart, F., Ardilouze, C., Bonet, A., Brookshaw, A., Chen, M., Codorean, C., et al. (2017). The subseasonal to seasonal (S2S) prediction project database. *Bulletin of the American Meteorological Society*, *98*(1), 163–173. https://doi.org/10.1175/bams-d-16-0017.1

Waliser, D., Sperber, K., Hendon, H., Kim, D., Maloney, E., Wheeler, M., et al. (2009). MJO simulation diagnostics. *Journal of Climate*, *22*(11), 3006–3030.
Waliser, D. E., Lau, K. M., Stern, W., & Jones, C. (2003). Potential predictability of the Madden–Julian oscillation. *Bulletin of the American Meteorological Society*, *84*(1), 33–50. https://doi.org/10.1175/bams-84-1-33
Wang, B., & Chen, G. (2017). A general theoretical framework for understanding essential dynamics of Madden–Julian oscillation. *Climate Dynamics*, *49*(7–8), 2309–2328. https://doi.org/10.1007/s00382-016-3448-1
Wang, B., Chen, G., & Liu, F. (2019). Diversity of the Madden-Julian oscillation. *Science Advances*, *5*(7), eaax0220. https://doi.org/10.1126/sciadv.aax0220
Wang, B., Liu, F., & Chen, G. (2016). A trio-interaction theory for Madden–Julian oscillation. *Geoscience Letters*, *3*, 1–16. https://doi.org/10.1186/s40562-016-0066-z
Wang, B., & Rui, H. (1990). Synoptic climatology of transient tropical intraseasonal convection anomalies: 1975–1985. *Meteorology and Atmospheric Physics*, *44*(1–4), 43–61. https://doi.org/10.1007/bf01026810
Wang, B., & Wang, T. (2023). How the 1999 climate shift has changed MJO propagation diversity. *Journal of Climate*, *36*(10), 3523–3535. https://doi.org/10.1175/jcli-d-22-0749.1
Wang, B., & Xie, X. (1997). A model for the boreal summer intraseasonal oscillation. *Journal of the Atmospheric Sciences*, *54*(1), 72–86. https://doi.org/10.1175/1520-0469(1997)054<0072:amftbs>2.0.co;2
Wang, H., Liu, F., Wang, B., Chen, G., & Dong, W. (2021). Diversity of intraseasonal oscillation over the western North Pacific. *Climate Dynamics*, *57*(7–8), 1881–1893. https://doi.org/10.1007/s00382-021-05780-2
Wang, T., & Li, T. (2021). Factors controlling the diversities of MJO propagation and intensity. *Journal of Climate*, *34*(16), 6549–6563.
Wei, Y., Liu, F., Mu, M., & Ren, H. L. (2018). Planetary scale selection of the Madden–Julian Oscillation in an air-sea coupled dynamic moisture model. *Climate Dynamics*, *50*(9–10), 3441–3456. https://doi.org/10.1007/s00382-017-3816-5
Wei, Y., Liu, F., Ren, H. L., Chen, G., Feng, C., & Chen, B. (2022). Western Pacific premoistening for eastward-propagating BSISO and its ENSO modulation. *Journal of Climate*, *35*(15), 4979–4996. https://doi.org/10.1175/jcli-d-21-0923.1
Wei, Y., Mu, M., Ren, H. L., & Fu, J. X. (2019). Conditional nonlinear optimal perturbations of moisture triggering primary MJO initiation. *Geophysical Research Letters*, *46*(6), 3492–3501. https://doi.org/10.1029/2018gl081755
Wei, Y., & Pu, Z. (2021). Moisture variation with cloud effects during a BSISO over the eastern maritime continent in a cloud-permitting-scale simulation. *Journal of the Atmospheric Sciences*, *78*(6), 1869–1888. https://doi.org/10.1175/jas-d-20-0210.1
Wei, Y., & Ren, H. L. (2019). Modulation of ENSO on fast and slow MJO modes during boreal winter. *Journal of Climate*, *32*(21), 7483–7506. https://doi.org/10.1175/JCLI-D-19-0013.1
Wei, Y., & Ren, H. L. (2022). Distinct MJOs under the two types of La Niña. *Journal of Geophysical Research: Atmospheres*, *127*(23), e2022JD037646. https://doi.org/10.1029/2022jd037646
Wei, Y., Ren, H. L., Mu, M., & Fu, J. X. (2020). Nonlinear optimal moisture perturbations as excitation of primary MJO events in a hybrid coupled climate model. *Climate Dynamics*, *54*(1–2), 675–699. https://doi.org/10.1007/s00382-019-05021-7
Wei, Y., Ren, H. L., Xiang, B., Wang, Y., Wu, J., & Wang, S. (2023). Diverse MJO Genesis and predictability. *Bulletin of the American Meteorological Society*, *104*(4), E792–E809. https://doi.org/10.1175/bams-d-22-0101.1
Xiang, B., Harris, L., Delworth, T. L., Wang, B., Chen, G., Chen, J. H., et al. (2021). *S2S prediction in GFDL SPEAR: MJO diversity and teleconnections* (pp. 1–46). Bulletin of the American Meteorological Society.
Yadav, P., & Straus, D. M. (2017). Circulation response to fast and slow MJO episodes. *Monthly Weather Review*, *145*(5), 1577–1596. https://doi.org/10.1175/mwr-d-16-0352.1
Zhang, C. (2005). Madden-Julian oscillation. *Reviews of Geophysics*, *43*(2). https://doi.org/10.1029/2004rg000158
Zhang, C. (2013). Madden–Julian oscillation: Bridging weather and climate. *Bulletin of the American Meteorological Society*, *94*(12), 1849–1870. https://doi.org/10.1175/bams-d-12-00026.1
Zhang, C., Adames, Á. F., Khouider, B., Wang, B., & Yang, D. (2020). Four theories of the Madden-Julian oscillation. *Reviews of Geophysics*, *58*(3), e2019RG000685. https://doi.org/10.1029/2019rg000685
Zhang, C., & Ling, J. (2017). Barrier effect of the Indo-Pacific Maritime Continent on the MJO: Perspectives from tracking MJO precipitation. *Journal of Climate*, *30*(9), 3439–3459. https://doi.org/10.1175/jcli-d-16-0614.1
Zhang, C., & Yoneyama, K. (2017). CINDY/DYNAMO field campaign: Advancing our understanding of MJO initiation. In *The global monsoon system: Research and forecast* (pp. 339–348).
Zhao, C., Li, T., & Zhou, T. (2013). Precursor signals and processes associated with MJO initiation over the tropical Indian Ocean. *Journal of Climate*, *26*(1), 291–307. https://doi.org/10.1175/jcli-d-12-00113.1
Zhou, L., & Murtugudde, R. (2020). Oceanic impacts on MJOs detouring near the Maritime Continent. *Journal of Climate*, *33*(6), 2371–2388. https://doi.org/10.1175/jcli-d-19-0505.1

References From the Supporting Information

Chen, X., Ling, J., & Li, C. (2016). Evolution of the Madden-Julian Oscillation in two types of El Niño. *Journal of Climate*, *29*(5), 1919–1934. https://doi.org/10.1175/jcli-d-15-0486.1
Liu, F., Li, T., Wang, H., Deng, L., & Zhang, Y. (2016). Modulation of boreal summer intraseasonal oscillations over the western North Pacific by ENSO. *Journal of Climate*, *29*(20), 7189–7201. https://doi.org/10.1175/jcli-d-15-0831.1
Liu, F., Wang, B., Ouyang, Y., Wang, H., Qiao, S., Chen, G., & Dong, W. (2022). Intraseasonal variability of global land monsoon precipitation and its recent trend. *Npj Climate and Atmospheric Science*, *5*(1), 30. https://doi.org/10.1038/s41612-022-00253-7
Wu, R., & Song, L. (2017). Spatiotemporal change of intraseasonal oscillation intensity over the tropical Indo-Pacific Ocean associated with El Niño and La Niña events. *Climate Dynamics*, *50*(3–4), 1221–1242. https://doi.org/10.1007/s00382-017-3675-0